ISGSR 2011 - Vogt, Schuppener, Straub & Bräu (eds) - © 2011 Bundesanstalt für Wasserbau ISBN 978-3-939230-01-4

Hydraulic Heave Safety at Excavations with Surcharge Filters

P. Schober & C. Boley
Bundeswehr University Munich, Neubiberg, Germany

B. Odenwald
Federal Waterways Engineering and Research Institute, Karlsruhe, Germany

ABSTRACT: When designing deep excavation pits next to waterways that are still being operated, verifying hydraulic heave safety is crucial to determine the necessary length of the pit walls. To reduce their embedment depth, a surcharge filter can be installed. However, studies based on numerical groundwater computations show that verification standards for hydraulic heave safety are not applicable for excavation pits with an installed surcharge filter. Standard approaches neglect significant vertical flow below the wall toe. A method which considers these flow forces was developed based on the numerical flow computations to determine reliably the necessary thickness of the surcharge filter. To examine this theoretical approach and the failure mechanism, several laboratory tests were performed which were evaluated with various methods.

Keywords: safety, groundwater, hydraulic heave, laboratory test, filter

1 INTRODUCTION

Installing deep excavation pits next to waterways which are still being operated has become a more and more frequent practice for construction measures to allow continued ship traffic. Verification of hydraulic heave safety is required to determine the length of the pit walls. To reduce the embedment depth of the walls, a surcharge filter can be installed at the pit bottom. Due to current construction measures on German waterways, the German Federal Waterways Engineering and Research Institute performed numerical groundwater flow computations. However, these brought up general questions on hydraulic heave safety in cases of a reduced embedment depth of the pit walls due to a surcharge filter installed inside the excavation pit. Odenwald and Herten (2008) already documented the results of the performed analyses in detail. Based on these, the Bundeswehr University Munich conducted comprehensive laboratory tests and evaluated these using various methods.

2 VERIFICATION OF HYDRAULIC HEAVE SAFETY

Lowering the groundwater level inside an excavation pit down to its bottom leads to groundwater flow to the excavation pit with an upward flow direction from the wall toe to the bottom of the excavation pit. If the thus caused flow force S suspends the buoyant weight of the soil G' as well as other possible stabilizing forces R, hydraulic heave results (Figure 1). This can lead quickly to the flooding of the excavation pit due to regressive erosion around the toe wall as well as to the collapse of the excavation pit.Based on the German geotechnical codes, hydraulic heave safety is verified according to approaches by Terzaghi-Peck (Terzaghi and Peck, 1948) or Baumgart-Davidenkoff (Davidenkoff, 1970). These use a simplified unstable block to determine the relevant forces. Both methods only compare the flow force S and the buoyant weight of the soil G'. Possible friction forces are neglected. Terzaghi-Peck's approach determines the forces with the help of a prismatic soil block whose height corresponds to the embedment depth t of the wall below the pit bottom and whose width corresponds to half of the embedment depth (b = t/2). Baumgart-Davidenkoff's approach uses a block whose width is negligible and whose height is

also the distance between the pit bottom and the wall toe. Since, in cases of undercurrent flow, the groundwater potential at the wall toe is always higher than the mean potential at the lower edge of the unstable block according to Terzaghi-Peck's approach, Baumgart-Davidenkoff's approach is always more conservative.

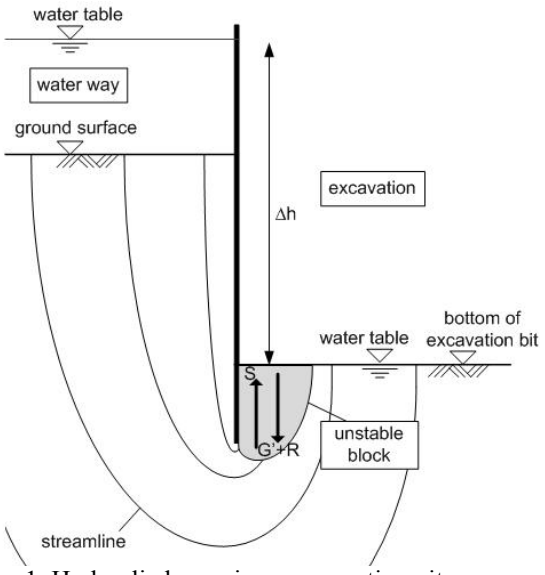

Figure 1. Hydraulic heave in an excavation pit

When using a surcharge filter, the height of the unstable block is the distance between the wall toe and the upper edge of the surcharge filter. The relevant width, however, according to Terzaghi and Peck (1948), corresponds only to a half of the embedment depth of the wall below the pit bottom. In this case, the weight of the surcharge filter needs to be considered as an additional stabilizing force. The installed surcharge filter needs to be filter stable against the soil below the pit bottom and may only cause a slight decrease of the groundwater potential. This means that the material used for the surcharge filter must be fine enough to prevent soil particles from being transported into the surcharge filter and coarse enough to allow the water penetrating the surcharge filter freely.

3 NUMERICAL GROUNDWATER FLOW COMPUTATIONS

3.1 *General*

The numerical groundwater flow computations were performed based on a steady state, vertical-plane groundwater model under simplified assumptions. This refers in particular to the assumptions of a groundwater potential at both sides of the pit wall at the height of the terrain or pit surface (below the surcharge filter) and of a homogeneous and isotropic ground. Thus, in cases of flow in direction of the pit, the groundwater potential can be described by only considering the quotient of the pit wall's embedment depth below the pit bottom and the groundwater potential difference Δh.

3.2 *Conventional approach*

According to Terzaghi-Peck's or Baumgart-Davidenkoff's approaches, the flow force results from the residual potential difference Δh_r between the lower edge of the unstable block at the wall toe and the pit bottom. Considering the applied simplified assumptions, the quotient of the residual potential difference and the total potential difference $\Delta h_r/\Delta h$ can be specified as a function of $t/\Delta h$ (Figure 2). As the length of the applied unstable block only corresponds to the distance from the pit bottom to the lower edge of the wall, the residual potential difference drops down to zero with decreasing embedment depth t. If an unstable block starting at the wall toe is used for the computations, vertical flow in the ground below the wall toe is not considered.

Applying the functional relation of $\Delta h_r/\Delta h$ and $t/\Delta h$ also allows determining the necessary thickness of the surcharge filter d_F depending on $t/\Delta h$. For the equilibrium state without any safety factors, a dimensionless variable including the quotients $d_F/\Delta h$ and γ_F/γ_W (γ_F: unit weight of the surcharge filter material; γ_W: unit weight of water) is specified for a ratio $\gamma_S'/\gamma_W = 1.0$ (γ_S' buoyant unit weight of the soil) depending on $t/\Delta h$ (Figure 3). As expected, according to the two approaches by Terzaghi-Peck and Baumgart-

Davidenkoff, the necessary filter thickness initially rises with constant potential difference and decreasing embedment depth. After reaching a maximum, however, the necessary filter thickness drops with constant potential difference and continuously decreasing embedment depth down to zero. Apparently, verifying hydraulic heave safety for a construction which involves a surcharge filter by using an unstable block that only reaches to the wall toe is inadequate to determine the necessary wall embedment in the ground.

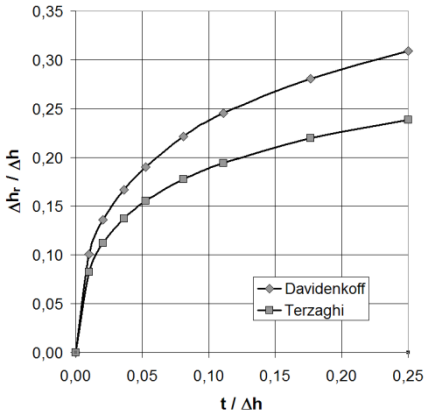

Figure 2. Residual potential difference Δh_r

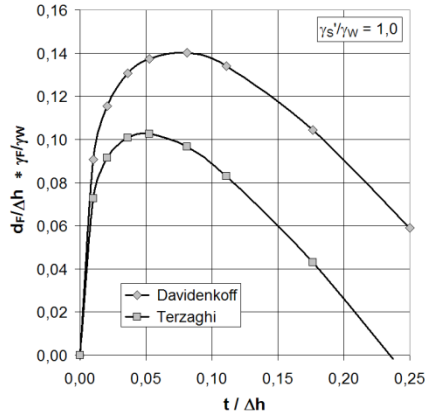

Figure 3. Required thickness of the surcharge filter d_F

3.3 *Approach with an extended unstable block*

The analyzed undercurrent flow below the walls of an excavation pit included flow in an upward direction below the wall toe. The performed numerical computations showed that in case of a surcharge filter installed on top of the pit bottom and pit walls with reduced embedment depth, significant vertical gradients may develop below the pit bottom, which partially lie significantly above the limiting gradient $i_{gr} = \gamma_S'/\gamma_W$.

To determine an unstable block which considers vertical flow in the ground in a sufficient manner, an area below the wall toe needs to be defined where the vertical component of the specific hydraulic gradient i_z is higher than the limiting gradient i_{gr}. Below this area, the specific soil weight is always higher than the specific flow force, so, for the verification of hydraulic heave safety, the equilibrium in this area is not exceeded. Hydraulic heave safety needs to be verified based on an unstable block that also covers the distance between the wall toe and the critical depth ($i_z = i_{gr}$). In the following, the new verification approach (based on Baumgart-Davidenkoff's approach) which involves the adapted unstable block is illustrated.

Using the extended unstable block, a corrected residual potential difference can be determined. This time, we did not consider the distance between the wall toe and the pit bottom but the distance between the critical depth ($i_z = i_{gr}$) below the wall toe and the pit bottom. The functional relation between the necessary thickness of the surcharge filter relating to the total potential difference $d_F/\Delta h$ and the quotient of embedment depth and potential difference $t/\Delta h$ can be determined in the same way as for the conventional unstable block. This is illustrated in Figure 4 for the equilibrium state and a quotient of the buoyant unit weight of the soil and the unit weight of water $\gamma_S'/\gamma_W = 1.0$. As opposed to the approach using an unstable block that starts at the wall toe, computations based on the new approach, using an extended unstable block, concluded that even if the embedment depth is reduced down to zero a surcharge filter is still needed. However, a maximum is also reached here, which means that at constant potential difference, a further reduction of the embedment depth requires a less thickness of the surcharge filter. To verify this apparently contradictory statement, laboratory tests were performed that are described in the following.

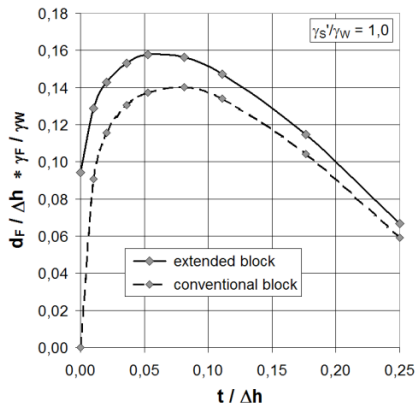

Figure 4. Required thickness of the surcharge layer d_F (conventional and extended unstable block)

The detailed computation basis for the verification of hydraulic heave safety using the method described above, also regarding relevant safety factors, as well as the determination of the necessary dimensions of the surcharge filter, with or without considering friction forces in the filter material, were described by Odenwald and Herten (2008).

4 VISUALIZATION OF FAILURE BY LABORATORY TESTS

To verify the theoretical approach, the Institute for Soil Mechanics and Geotechnical Engineering of the Bundeswehr University Munich carried out numerous laboratory tests in a specific box to simulate hydraulic heaves. During the experimental series, the embedment depth t of the wall and the thickness of the surcharge filter d_F were varied. Moreover, the elevations on the inside of the wall were detected by displacement transducers, the water pressure around the base of the partition panel was measured by water pressure sensors and the figure of failure was mapped by the Particle Image Velocimetry (PIV) method and video recording.

4.1 *Construction and design of experimental rig*

To visualize the fracture behavior and to verify the theoretical approach, we designed a specific apparatus to simulate hydraulic heaves (Figure 5). The test rig consists of two parts: the water supply, which is used to increase the potential difference continuously, and the test box. The water supply is delivered by a box with an installed overfall and a staff gauge to regulate the potential difference. The water supply and the test box were connected by a pipe (∅ 3 cm) and placed on a hand lift truck to change the potential difference continuously.

The rectangular test box has the following dimensions: length x width x height = 1.70 m x 0.40 m x 1.50 m. It consists mainly of 4 acrylic glass walls, a base plate and a vertically moveable partition acryl panel in the middle of the box. The partition wall simulates the retaining wall in the laboratory test. An inlet connects the test box with the water supply. On the feed stream side of the test box, 3 pipes, each with an internal diameter of 3 cm, allow free drain. To be able to distribute the sand homogeneously and in the default effective density, the test box can be split at a height of 90 cm, measured from the bottom. After filling in the sand, the test box can be sealed.

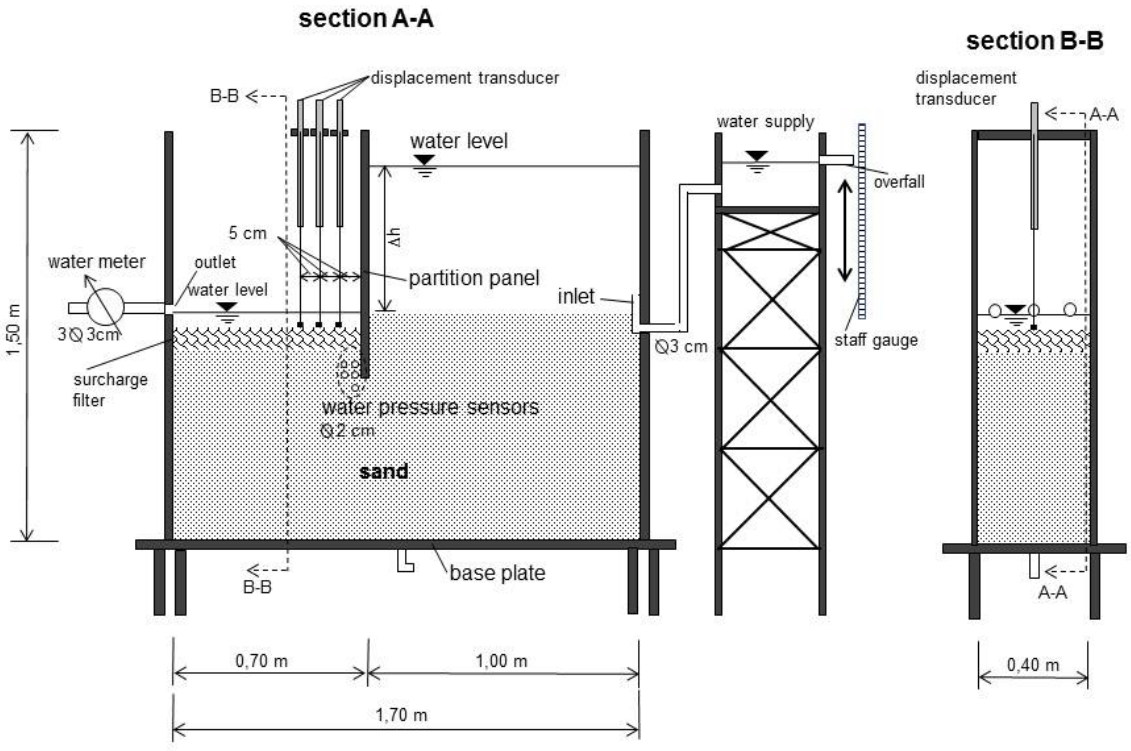

Figure 5. Construction of experimental rig

4.2 *Description of test material*

Sand (as basic material) and a mixture of coarse sand and fine gravel (as filter material) were used as test material for the simulations of hydraulic heave with filter layers at the excavation side of the wall.

As basic material, sand with a closeness of grain ρ_s = 2.72 g/cm³ and a grain size distribution of 0.1 mm to1 mm was used. The test sand can be classified as uniform fine- to medium-graded sand. The coefficient of permeability (k_f) was determined as $k_f = 5.83 \times 10^{-5}$ m/s.

The surcharge filter consists of coarse sand and fine gravel with a closeness of grain ρ_s = 2,70 g/cm³ and with a grain size distribution from 0.6 mm to 7 mm. For the selection of the filter material, the filter rule according to Terzaghi was chosen.

4.3 *Installation of test material and description of test procedure*

The sand was filled into the test box in 2 cm thick layers. To reach the default effective density D = 0.8, the dry mass per layer had to be determined. For one layer with an effective density D = 0.8, a dry mass m_d = 22.2 kg was required. The sand was filled into the box underwater and was compacted by a stemmer. The height of one layer of sand was checked with the help of marks placed on the walls of the test box.

The surcharge filter was filled into the test box similar to the sand, with a default effective density D = 0.8 and in 2 cm thick layers. The required dry mass m_d per layer (in front of the partition panel) was determined as m_d = 9.2 kg.

Altogether, we carried out 18 tests. The embedment depth t was varied between t = 0 and t = 8 cm in 1 cm steps. Moreover, the surcharge filter was installed in three different sizes, with a thickness d_F = 2, 4 and 6 cm. In the test series, the different embedment depths of the wall were combined with the three different sizes d_F of the surcharge filter.

At the beginning of each test, the water level on both sides of the partition panel was equal. Hence, there were no flow forces acting on the sand. The test was started by switching on all measuring instruments at the same time. This was necessary to permit a direct comparison of all measurement techniques. At first, the potential difference Δh was raised by 10 cm. In each of the following steps, it was further raised by 2 cm. This procedure was repeated until hydraulic heave occurred. The duration of one step was defined individually by using the measuring curves from the water pressure sensors. When the potential curves of the water pressure sensors were deflected after an increase of the potential difference Δh, it was assumed that a steady flow had occurred. At this point the next potential step was introduced.

4.4 *Experimental observations of failure mode*

We observed the failure mode of the hydraulic heave during the test series using several measurement techniques. The used measuring instruments and techniques were:

- 3 water pressure sensors around the base of the partition panel
- 3 displacement sensors in the middle of the test box
- fluid flow meter behind the outlet of the test box
- Particle Image Velocimetry (PIV) method

Two different temporal failure processes of hydraulic heave, depending on the thickness of the surcharge filter d_F, were observed. During the tests with a thickness of the surcharge filter d_F = 2 cm, relevant elevations were already detected some potential steps before the hydraulic heave occurred. As for the tests with the surcharge filter sizes d_F = 4 cm or d_F = 6 cm, the hydraulic heave occurred 1 to 3 minutes after the first elevation could be observed. Therefore, it can be assumed that the thickness of the surcharge filter d_F has a significant influence on the fracture behavior.

4.4.1 *Illustration of failure figure by Particle Image Velocimetry (PIV) method*

During these laboratory experiments, we observed fracture mechanics with the PIV method. Small displacements of the sand could be identified and their direction and amplitude could be determined. Figure 6 shows absolute displacements around the base of the partition panel for different potential differences with an embedment depth t of 4 cm and a thickness of the surcharge filter d_F of also 4 cm.

Figure 6 underlines that the displacements begin under the base of the partition panel at a potential difference Δh of 42 cm. Later on, the displacements spread to the downstream side of the partition panel (Δh = 46 - 50 cm). If the uplift on the upstream site of the panel has a certain value, the displacements spread

to the backside of the wall and the hydraulic heave is initiated (Δh = 50 cm - 54 cm). The same failure behavior was observed in almost all tests.

Furthermore, the yield line of the unstable block can be visualized by the PIV method for all potential differences. Hence, the geometry of the unstable block for several potential differences Δh can be determined. For further investigation, the results of the analysis can be used as a basis to develop the theoretical approach and adapt the unstable block.

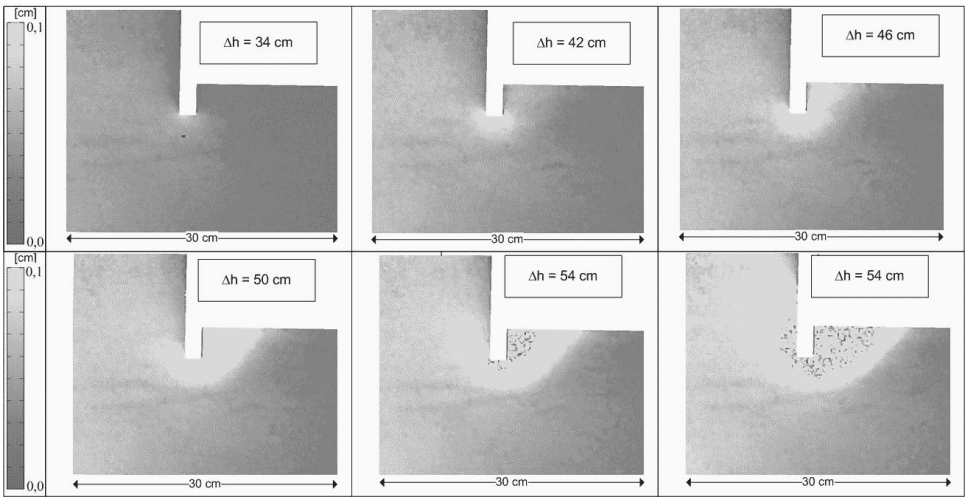

Figure 6. Absolute displacements around the base of the partition panel for different potential differences

4.4.2 *Vertical displacements in front of the partition wall*

Figure 7 shows vertical displacements on the surface of the sand in front of the partition panel measured by the PIV method. The diagram shows that the first significant vertical elevations happen at the potential difference of Δh = 50 cm. This corresponds to the results illustrated in Figure 6 which show that the significant displacements at the downstream of the partition panel start at the same potential difference. Furthermore, the diagram visualizes the shape and the length of the unstable block. In this test the maximum length of the unstable block, briefly before the hydraulic heave occurs, is about 13 cm.

Figure 8 shows vertical displacements on the surface of the surcharge filter in the middle of the test box. The displacements were detected by displacement transducers. Transducer 1, which is located at a distance from the partition panel of 5 cm, also shows the first significant elevations at the potential difference of Δh = 48 cm - 50 cm. This corresponds to the observations in Figure 7.

Transducer 2, at a distance of 10 cm from the partition panel, displays smaller elevations than transducer 1. However, the significant elevations begin at a potential difference of Δh = 52 cm. Transducer 3, at a distance of 15 cm from the partition panel, displays no significant elevations. This conforms to the results in Figure 7, where the displacements in a distance of 15 cm to the partition panel are also zero.

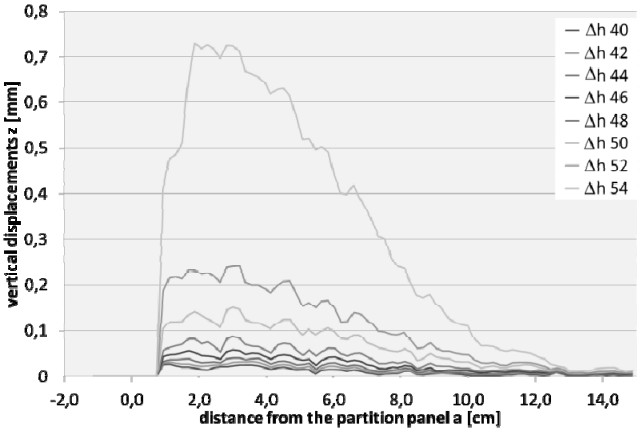

Figure 7. Vertical displacements z [mm] at the sand surface (PIV)

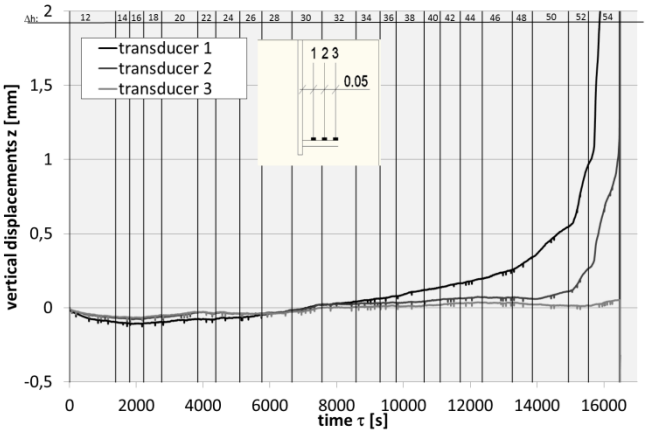

Figure 8. Vertical displacements z [mm] at the filter surface (transducer)

Additionally, the phenomenon of bulking could be observed during the test series. Figure 9 shows the bulking of the sand in front the partition panel for the test with an embedment depth t of 2 cm and a thickness of the surcharge filter d_F of 6 cm.

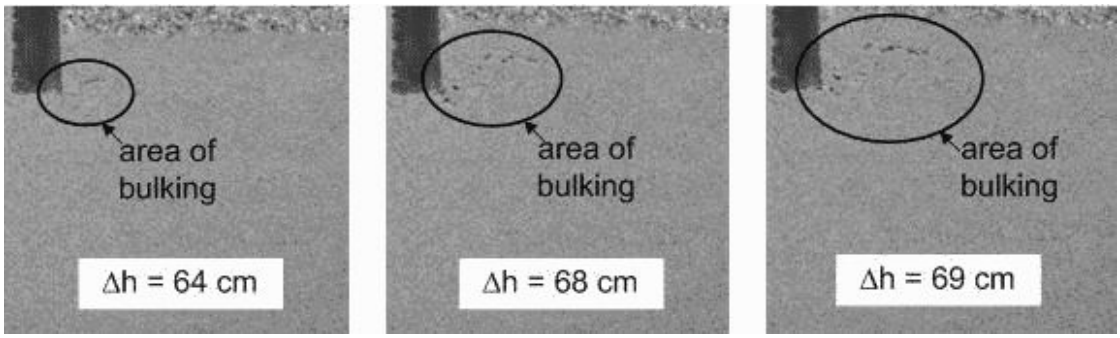

Figure 9. Bulking of sand in front of the partition panel

4.4.3 *Water pressure conditions around the base of the partition wall and flow rate*

The water pressure around the base of the partition wall was detected during each test by 3 water pressure sensors. The recorded pressure curves were used to control the duration of a potential step. Comparing the curves of the water pressure sensors with the illustration of the absolute displacements detected with the PIV method (Figure 6), it can be seen that the displacements at the base of the partition panel occur at the potential difference of $\Delta h = 42$ cm where the irregular run of the curves begins. Hence, relocations and/or displacements in the test sand can be detected by observing water pressure curves. Figure 10 shows the curves for the test with an embedment depth t of 4 cm and a thickness of the surcharge filter d_F of also 4 cm. The position of the water pressure sensors also is shown in Figure 10. At the beginning of the test, the hydraulic differences are relatively small. Hence, no relocations or displacements occur and the pressure curves run regularly ($\Delta h = 12$ cm – 38 cm in Figure 10). If the curves show jerky leaps or run irregularly, it can be assumed that relocations and/or displacements occur around the pressure sensor ($\Delta h = 38$ cm – 54 cm in Figure 10).

Figure 11 illustrates the flow rate in [l/min] for each potential step (with an embedment depth t of 4 cm and a thickness of the surcharge filter d_F of 4 cm). It can be seen that the rise of the flow rate is in a linear relation with the potential difference Δh. Hence, the permeability does not increase during the test even if relocation and/or displacements occur.

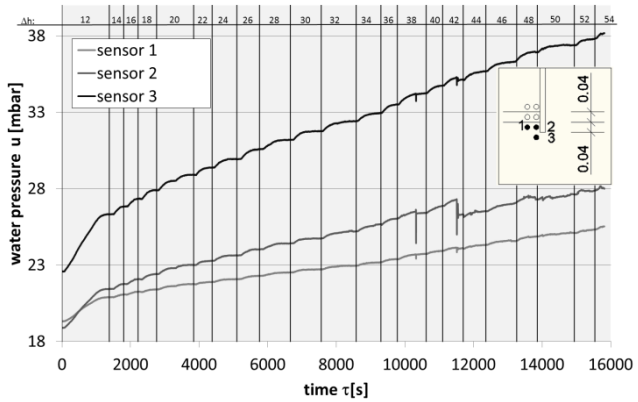

Figure 10. Water pressure u [mbar]

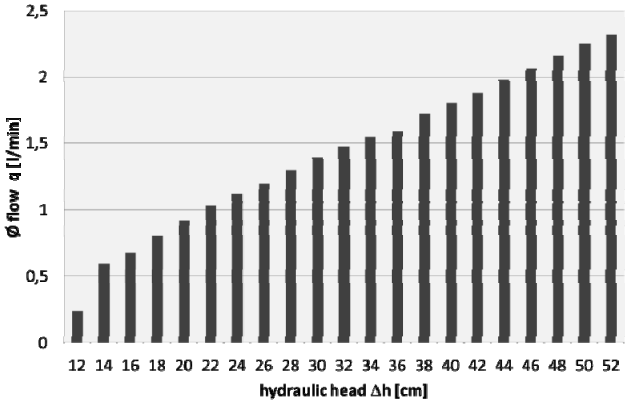

Figure 11. Flow rate for each potential step [l/min]

4.5 *Results of experiments*

Figure 12 shows the results of the experimental series and the theoretical approach as a function of $d_F/\Delta h$ and $t/\Delta h$. Similar to the results of the theoretical approach, the test results show that the required thickness of the surcharge filter d_F drops down from a defined ratio between the embedment depth of the wall and the potential difference $t/\Delta h$.

The results of the test series are clearly below the results of the theoretical approach. Hence, the theoretical approach can be assessed as being very conservative. In the theoretical approach, only the weight of the unstable block is considered. The assumption and the idealized unstable block in the theoretical approach cause the differences between the theoretical approach and the experimental tests.

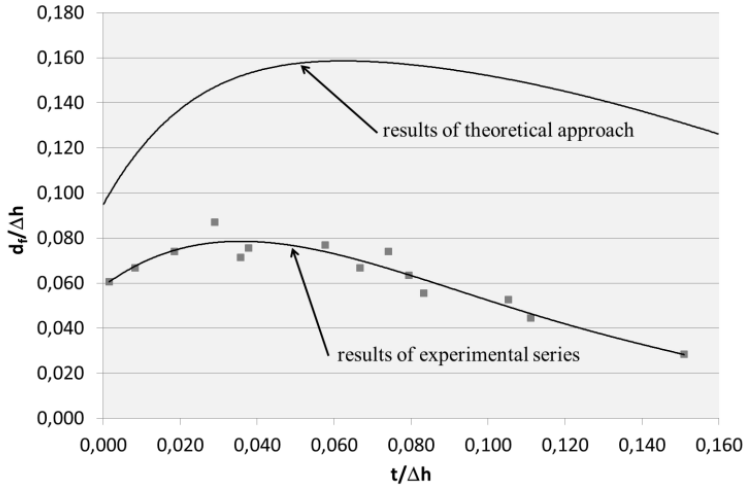

Figure 12. Results of experimental series as a function of $d_F/\Delta h$ and $t/\Delta h$

The theoretical and experimental series both prove that the hydraulic heave safety increases if the embedded depth of the wall is very small. Figure 13 illustrates this phenomenon clearly. For the test with an embedment depth t = 4 cm, a maximum potential difference Δh = 52 cm was reached. In comparison, for an embedment depth t = 0 cm, a maximum potential difference of Δh = 66 cm was reached. Although the embedment depth t was reduced 4 cm, the maximum potential difference Δh was 14 cm higher. The mechanical approach of this phenomenon will be object to further investigation.

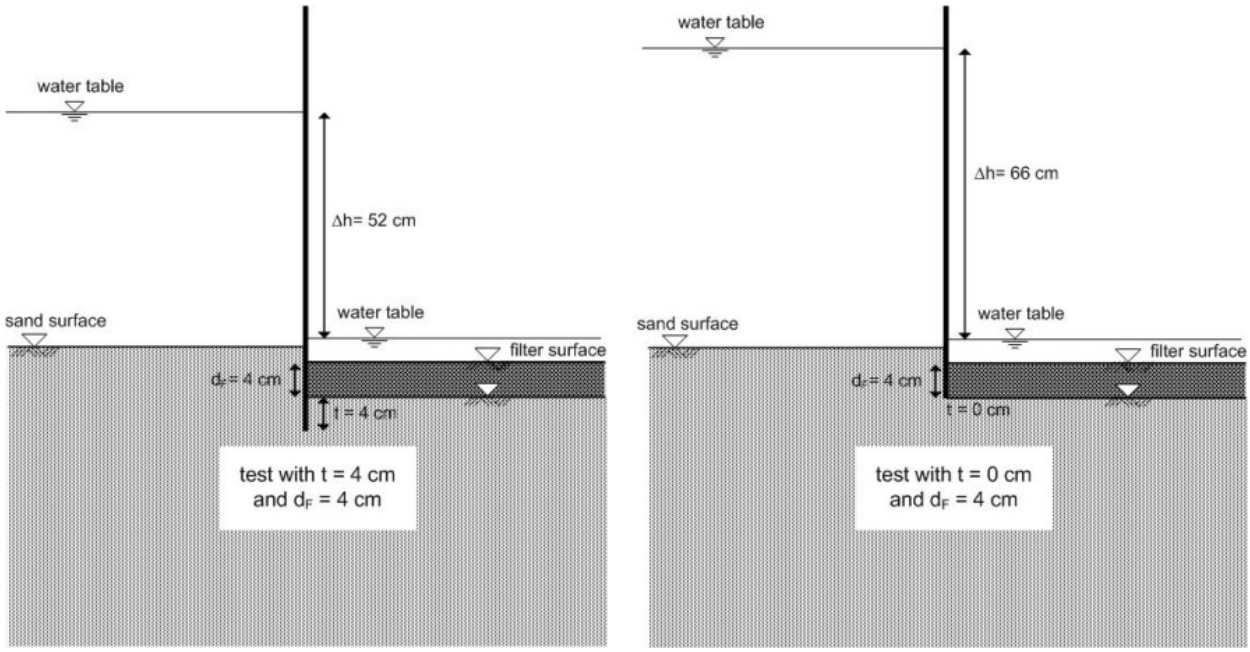

Figure 13. Illustration of the measured potential difference Δh for the tests with t = 4 cm and t = 0 cm (d_F = 4 cm)

5 CONCLUSION

The result of the numerical computation with an extended unstable block and the results of the experimental series show qualitatively similar results. If the ratio between the embedment depth of the wall and the potential difference $t/\Delta h$ falls below a defined value, the required thickness of the surcharge filter d_F drops. With the applied measurement techniques, the failure figure could be visualized and the failure mode was observed.

REFERENCES

Davidenkoff, R., 1970. Unterläufigkeit von Stauwerken, Wernerverlag, Düsseldorf
Odenwald, B., Herten, M., 2008. Hydraulischer Grundbruch: neue Erkenntnisse, Bautechnik 85, Heft 9, S. 585 -595
Terzaghi, K, Peck, R. B., 1948. Soil Mechanics in Engineering Practice, John Wiley and Sons, New York